

Influence of the Heteroatom Size on the Redox Potentials of Selected Polyoxoanions

Israël-Martyr Mbomekallé,^{*,†} Xavier López,^{*,‡} Josep M. Poblet,[‡] Francis Sécheresse,[†] Bineta Keita,[§] and Louis Nadjo[§]

[†]Institut Lavoisier, UMR 8180, Université de Versailles St. Quentin, 45 Avenue des Etats-Unis, 78035 Versailles Cedex, France, [‡]Departament de Química Física i Inorgànica, Universitat Rovira i Virgili, Marcel·li Domingo s/n, 43007 Tarragona, Spain, and [§]Laboratoire de Chimie Physique, Electrochimie et Photoélectrochimie, Université Paris-Sud, UMR 8000, CNRS, Orsay F-91405, France

Received April 9, 2010

The apparent formal potentials for the one-electron redox process of most Keggin-type heteropolytungstates, $XW_{12}O_{40}^{q-}$, have long been shown to linearly depend on their overall negative charges, in the absence of proton interference in the process. However, for a given overall negative charge, these formal potentials are also shown here to depend on the specific central heteroatom X. In the present work, cyclic voltammetry was used to study a large variety of Keggin-type anions, under conditions where their comparisons are straightforward. In short, apparent potential values get more negative (the clusters are more difficult to reduce) for smaller central heteroatoms within a given family of Keggin-type heteropolyanions carrying the same overall negative charge. Density functional theory calculations were performed on the same family of Keggin compounds and satisfactorily reproduce these trends. They show that internal XO_4 units affect differently the tungstate oxide cage. The electrostatic potential created by each internal anionic unit in a fragment-like approach ($XO_4^{q-}@W_{12}O_{36}$) was analyzed, and it is observed that X atoms of the same group show slight differences. Within each group of the periodic table, X atoms with lower atomic numbers are also smaller in size. The net effect of such a tendency is to produce a more negative potential in the surroundings and thus a smaller capacity to accept electrons. The case of $[BW_{12}O_{40}]^{5-}$ illustrates well this conclusion, with the smallest heteroatom of the Keggin series with group III central elements and a very negative reduction potential with respect to the other elements of the same group. Particularly in this case, the electronic structure of the Keggin anion shows the effects of the small size of boron: the highest occupied molecular orbitals of $[BW_{12}O_{40}]^{5-}$ appear to be ~ 0.35 eV higher than those in the other clusters of the same charge, explaining that the BO_4 unit is more unstable than AlO_4 or GaO_4 despite carrying the same formal charge.

Introduction

Polyoxometalates (POMs for short) are early-transition-metal anionic molecular nanoclusters that simultaneously exhibit many properties that make them attractive for applications in catalysis, separations, imaging, materials science,

and medicine. The chemistry of POMs¹ has become a very rich field, especially since the 1960s, and is still in constant academic and technological development.² With the recently summarized pioneering work of Baker and co-workers,³ the study of the properties of POMs entered an era of systematic investigation that continues unabated. Among the plethora of beneficial properties, the importance of redox behaviors was soon recognized. In this domain, simple rules could be rapidly established. Keeping, for clarity, with Keggin-type $XW_{12}O_{40}^{q-}$ anions, the following main parameters appear to govern their voltammetric behaviors: (i) the basicity of the first reduced species and, occasionally, of the fully oxidized species; (ii) the overall negative charge of the POM, which is a function of the central heteroatom charge; (iii) the size of this central heteroatom; (iv) finally, it is worth noting that, in the vast majority of the most studied Keggin-type POMs, the

*To whom correspondence should be addressed. E-mail: Israel.mbomekalle@chimie.uvsq.fr (I.-M.M.), javier.lopez@urv.cat (X.L.).

(1) Pope, M. T. *Heteropoly and Isopoly Oxometalates*; Springer-Verlag: Berlin, 1983.

(2) (a) Pope, M. T.; Müller, A. *Angew. Chem., Int. Ed.* **1991**, *30*, 34. (b) Pope, M. T.; Müller, A. *Polyoxometalates: From Platonic Solids to Antiretroviral Activity*; Kluwer: Dordrecht, The Netherlands, 1994. (c) Pope, M. T.; Müller, A. *Polyoxometalate Chemistry: From Topology via Self-Assembly to Applications*; Kluwer: Dordrecht, The Netherlands, 2001. (d) Hill, C. L. *Chem. Rev.* **1998**, *98*, 1. (e) Long, D.-L.; Burkholder, E.; Cronin, L. *Chem. Soc. Rev.* **2007**, *36*, 105. (f) Yamase, T.; Pope, M. T., Eds. *Polyoxometalate Chemistry for Nanocomposite Design*; Kluwer Academic: New York, 2002. (e) Keita, B.; Nadjo, L. In *Electrochemistry of Polyoxometalates, Encyclopedia of Electrochemistry*; Bard, A. J., Stratmann, M., Eds.; Wiley-VCH: New York, 2006; Vol. 7, pp 607–700.

(3) Baker, L. C. W.; Glick, D. C. *Chem. Rev.* **1998**, *98*, 3–49.

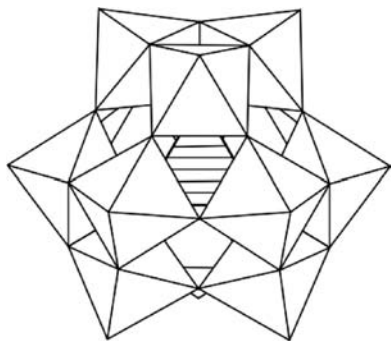


Figure 1. Polyhedral view of the α -Keggin structure. White octahedra and striped tetrahedra correspond to WO_6 and XO_4 units, respectively.

central heteroatom, X, is not electroactive, and we are mostly concerned with the redox behaviors of the addenda atoms. In this context, Pope and co-workers^{4–6} established that the one-electron redox potentials of Keggin $\text{XW}_{12}\text{O}_{40}^{q-}$ anions are a linear function of their overall charge, in the absence of proton interference in the process.⁴ Since then, electron addition in Keggin anionic species (shown in Figure 1), as well as other POM species,^{7,8} has carefully been investigated from both the experimental^{2c} and theoretical⁹ points of view. However, to our knowledge, the physical and/or electronic factors that govern the energetics of the first electron-transfer process in POM electrochemistry are not yet completely elucidated. The aim of the present work is to propose an answer to this question in the case where only electron transfer is involved. For this purpose, a large series of Keggin-type anions with different central heteroatoms were synthesized and studied under conditions in which a proton does not interfere with the electron-transfer process. Indeed, the influence of X has been studied, especially comparing the effect when X of different groups of the periodic table (i.e., P–Si–Al) is considered.^{4–6,10} In contrast, this work will compare variations of the redox potentials upon changes in X of the same group (P–As, Si–Ge, and B–Al–Ga). A few decades ago, Pope and co-workers observed small influences of the central heteroatom on the redox potentials of Keggin anions with the same electrical charge, but no thorough study that could explain this phenomenon was done.^{10e} More recently, Eda et al. reported that the first redox potential linearly depends on charge density calculated from the “real” size of the POM molecule.^{10f} In their study, the charge density was calculated for each Keggin compound by dividing its charge by the average volume value V , which is, of course, the same for all Keggin anions. They confirmed Pope’s results, but still no clear explanation was found for differences observed on the redox potentials of compounds with the same charge.

We herein combine cyclic voltammetry measurements with quantum mechanical calculations to clearly explain, for the first time, variations encountered in the redox potentials of POM compounds with different heteroatoms (X in the molecular formula $\text{XW}_{12}\text{O}_{40}$) of the same group of the periodic table.

Experimental Section

All compounds studied were prepared according to published methods¹⁰ and were characterized by Fourier transform infrared (FTIR) spectroscopy and electrochemistry. The IR spectra were recorded with KBr pellets on a Nicolet Magna IR 550 spectrophotometer. Pure water was used throughout. Water was purified by passing it through a RiOs 8 unit followed by a Millipore-Q Academic purification set. All reagents were of high-purity grade and were used as purchased without further purification. All cyclic voltammograms (CVs) were recorded at a scan rate of 10 mV s^{-1} , unless otherwise stated, on 0.5 mM solutions of the relevant polyanion. The compositions of the various media were as follows: for pH 0.5, 1.0, 2.0, and 3.0, 0.2 M $\text{Na}_2\text{SO}_4 + \text{H}_2\text{SO}_4$; for pH 4 and 5, 0.4 M $\text{CH}_3\text{COONa} + \text{CH}_3\text{COOH}$; for pH 6 and 7, 0.4 M $\text{NaH}_2\text{PO}_4 + \text{NaOH}$. The solutions were deaerated thoroughly for at least 30 min with pure argon and kept under a positive pressure of this gas during the experiments. The source, mounting, and polishing of the glassy carbon (GC; Le Carbone Lorraine, France) electrodes have been described.¹¹ The GC samples had a diameter of 3 mm. The electrochemical setup was an EG&G 273 A driven by a PC with the M270 software. Potentials are quoted against a saturated calomel electrode (SCE). The counter electrode was platinum gauze of a large surface area. All experiments were performed at room temperature, which is controlled and fixed for the laboratory at 20°C . Results were very reproducible from one experiment to another, and slight variations observed over successive runs are rather attributed to the uncertainty associated with the detection limit of our equipment (potentiostat, hardware, and software) and not to temperature variations, which are negligible anyway. The uncertainty in the redox potential values as measured on different CVs recorded under these working conditions is evaluated to be equal to 4 mV.

Results and Discussion

Re-exploration of the Electrochemical Behavior of Selected Heteropolytungstates in Solution. All of the polyanions used for our measurements are α isomers, according to the Baker and Figgis definition.¹² β - $[\text{AlW}_{12}\text{O}_{40}]^{5-}$ was also used for comparison with its parent α isomer. Cyclic voltammetry and controlled potential coulometry, when necessary, were used to revisit the electrochemical behavior of each compound in an aqueous solution at pH values in which the selected compound is stable enough to be characterized. To keep the overall negative charge of the POMs constant in each series, the study compares the redox behaviors of selected Keggin heteropolytungstates, whose central heteroatom belongs to the same group of the periodic table. The four different families of Keggin anions studied in this work according to the group number of the central heteroatom and thus their electrical charge are gathered in Table 1. We found that the requirements of stability and one-electron reversible reduction are fulfilled for all of the compounds in a pH 5 medium. However,

(4) Pope, M. T.; Varga, G. M., Jr. *Inorg. Chem.* **1966**, *5*, 1249–1254.

(5) Pope, M. T.; Papaconstantinou, E. *Inorg. Chem.* **1967**, *6*, 1147–1152.

(6) Papaconstantinou, E.; Pope, M. T. *Inorg. Chem.* **1967**, *6*, 1152–1155.

(7) Ortgea, F.; Pope, M. T. *Inorg. Chem.* **1984**, *23*, 3292–3297.

(8) Alizadeh, M. H.; Harmalkar, S. P.; Jeannin, Y.; Martin-Frère, J.;

Pope, M. T. *J. Am. Chem. Soc.* **1985**, *107*, 2662–2669.

(9) Poblet, J. M.; López, X.; Bo, C. *Chem. Soc. Rev.* **2003**, *32*, 297–308.

(10) (a) Souchay, P. *Ions minéraux condensés*; Masson et Cie: Paris, 1969;

p92. (b) Rocchiccioli-Deltcheff, C.; Fournier, M.; Franck, R.; Thouvenot, R.

Inorg. Chem. **1983**, *22*, 207–216. (c) Weinstock, I. A.; Cowan, J. J.; Barbuzzi,

E. M. G.; Zeng, H.; Hill, C. L. *J. Am. Chem. Soc.* **1999**, *121*, 4608–4617.

(d) Sundaram, K. M.; Neiwert, W. A.; Hill, C. L.; Weinstock, I. A. *Inorg. Chem.*

2006, *45*, 958–960. (e) Altenau, J. J.; Pope, M. T.; Prados, R. A.; So, H. *Inorg.*

Chem. **1975**, *14*, 417–421. (f) Eda, K.; Maeda, S.; Himeno, S.; Hori, T.

Polyhedron **2009**, *28*, 4032–4038.

(11) Keita, B.; Nadjo, L. *J. Electroanal. Chem.* **1988**, *243*, 87–103.

(12) Baker, L. C. W.; Figgis, J. S. *J. Am. Chem. Soc.* **1970**, *92*, 3794–3797.

Table 1. Classification of Selected Keggin Compounds into Four Different Families According to the Group Number of the Central Heteroatom

Keggin I	Keggin III	Keggin IV	Keggin V
$[\text{H}_2\text{W}_{12}\text{O}_{40}]^{6-}$	$[\text{BW}_{12}\text{O}_{40}]^{5-}$ $[\text{AlW}_{12}\text{O}_{40}]^{5-}$ $[\text{GaW}_{12}\text{O}_{40}]^{5-}$	$[\text{SiW}_{12}\text{O}_{40}]^{4-}$ $[\text{GeW}_{12}\text{O}_{40}]^{4-}$	$[\text{PW}_{12}\text{O}_{40}]^{3-}$ $[\text{AsW}_{12}\text{O}_{40}]^{3-}$

Table 2. Apparent Potentials, $E^\circ = (E_{\text{pa}} + E_{\text{pc}})/2$, for the First One-Electron Redox Process of Selected Keggin Compounds at pH 5 (0.4 M $\text{CH}_3\text{COONa} + \text{CH}_3\text{COOH}$),^a and Volumetric Charge Densities for Each Compound^b

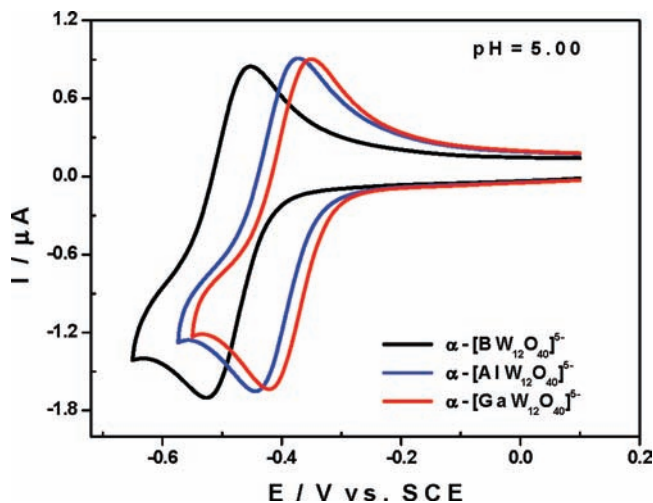
family	compound	volumetric density	E° (V)
Keggin I	$\alpha\text{-}[\text{H}_2\text{W}_{12}\text{O}_{40}]^{6-}$		-0.608
Keggin III	$\alpha\text{-}[\text{BW}_{12}\text{O}_{40}]^{5-}$	1.882	-0.491
	$\alpha\text{-}[\text{AlW}_{12}\text{O}_{40}]^{5-}$	1.868	-0.410
	$\alpha\text{-}[\text{GaW}_{12}\text{O}_{40}]^{5-}$	1.866	-0.387
Keggin IV	$\alpha\text{-}[\text{SiW}_{12}\text{O}_{40}]^{4-}$	1.506	-0.227
	$\alpha\text{-}[\text{GeW}_{12}\text{O}_{40}]^{4-}$	1.503	-0.190
Keggin V	$\alpha\text{-}[\text{PW}_{12}\text{O}_{40}]^{3-}$	1.138	+0.064
	$\alpha\text{-}[\text{AsW}_{12}\text{O}_{40}]^{3-}$	1.133	X

^a Potentials are quoted against a SCE reference electrode. Scan rate: 10 mV s^{-1} . Working electrode: GC. ^b The significance of the volumetric charge densities indicated in this table is issued from DFT calculations to be discussed later.

a complete re-exploration of the electrochemical behaviors of the selected heteropolytungstates was carried out at several pH values for the following reasons: (i) to compare the potentials measured exactly under the same conditions; (ii) occasionally, to check whether the same trends are maintained at several pH values in order to eliminate the interference of an eventual undetected initial protonation; (iii) to visit once more the voltammetric behavior of some clusters with a complex behavior like $[\text{BW}_{12}\text{O}_{40}]^{5-}$. Such detailed results are relegated to the Supporting Information (SI).

Table 2 gathers the apparent formal potentials, $E^\circ = (E_{\text{pa}} + E_{\text{pc}})/2$, for the first one-electron redox process of selected Keggin compounds at pH 5 (0.4 M $\text{CH}_3\text{COONa} + \text{CH}_3\text{COOH}$). The volumetric charge densities issued from the density functional theory (DFT) calculations are added and will be commented on later. A general trend emerges from the potential values quoted in this table: within a given family of heteropolyanions, i.e., Keggin compounds with the same overall negative charge, the apparent potential values get more negative (the clusters are more difficult to reduce) as the size of the central heteroatom reduces. It is worth noting that the observed trend is also found in several media, depending on the particular Keggin family (see the SI). Within each group of the periodic table, X atoms with lower atomic numbers are also smaller in size. This general trend is observed throughout the Keggin anion families (Table 2) and is illustrated in Figure 2, presented for the $\text{XW}_{12}\text{O}_{40}^{q-}$ anion series (X = B, Al, Ga).

The following qualitative reasoning might account for these observations. As has been previously proposed^{13–16} and applied,^{10c,17–19} many close-packed POMs may be

**Figure 2.** CVs of $\alpha\text{-}[\text{BW}_{12}\text{O}_{40}]^{5-}$ (black line), $\alpha\text{-}[\text{AlW}_{12}\text{O}_{40}]^{5-}$ (blue line), and $\alpha\text{-}[\text{GaW}_{12}\text{O}_{40}]^{5-}$ (red line) at pH 5.0. The scan is restricted to the first redox wave. POM concentration: 0.5 mM. Scan rate: 10 mV s^{-1} . Working electrode: GC. Reference electrode: SCE. For further details, see the SI.

seen as an internal anionic fragment surrounded by a neutral metal oxide cage, often expressed as $\text{XO}_4^{q-} @ \text{W}_{12}\text{O}_{36}$ for Keggin tungstates. This assumption permits the simplification of some features of these anions, such as some electronic properties. So, in order to explain the observations made on the redox potentials, we focus on the properties of the internal XO_4^{q-} units. This implies that the external neutral cages are virtually identical in all cases, and they cannot be at the origin of the experimental trends. Observation of $\text{W}_{12}\text{O}_{36}$ geometries reveals that they are very similar within a group of Keggin anions. In other words, the overall size of the Keggin anion remains nearly independent of the nature of the central heteroatom. Now, we focus on the bond sequence $\text{X}-\mu_4\text{-O}-\text{W}-\text{O}_t$, where O_t features a terminal oxygen atom. The aforementioned literature supports^{10c,13–19} established that the sum of $\text{X}-\mu_4\text{-O}$ and $\mu_4\text{-O}-\text{W}$ bond lengths remains constant while, in contrast, the size of the XO_4^{q-} unit changes with X. As a consequence, the $\mu_4\text{-O}-\text{W}$ bond length changes. The larger X is, the shorter the distance and the stronger the corresponding bond. Correlatively, the electron density will be high between the two atoms and the W atom will be partly depopulated of electrons. Because the W atom is the center and will receive the incoming electron in a reduction process, its reduction will be easier with larger X and vice versa. Such reasoning is also supported by the existence of a large difference between the electronegativities of the two bonded elements (3.44 for O and 2.36 for W).

DFT Calculations

In the search for a direct theoretical justification of the above reasoning, DFT calculations have been carried out on the $[\text{XW}_{12}\text{O}_{40}]^{q-}$ (X = B, Al, Ga, Si, Ge, P, As) series of compounds. The goal of these calculations is to find the physical origin for the observed redox potentials. In addition, theory might be helpful in identifying the better of the two parameters, equivalent in principle, to describe this physical origin, in terms of the electrical charge or electrostatic

(13) Clark, C. J.; Hall, D. *Acta Crystallogr.* **1976**, *B32*, 1454.

(14) Day, V. W.; Klemperer, W. G. *Science* **1985**, *228*, 533.

(15) Müller, A. *Nature* **1991**, *352*, 115.

(16) Pope, M. T. *Nature* **1992**, *355*, 27.

(17) Jansen, J. A.; Singh, D. J.; Wang, S.-H. *Chem. Mater.* **1994**, *6*, 146.

(18) Maestre, J. M.; López, X.; Bo, C.; Casañ-Pastor, N.; Poble, J. M. *J. Am. Chem. Soc.* **2001**, *123*, 3749–3758.

(19) López, X.; Maestre, J. M.; Bo, C.; Poble, J. M. *J. Am. Chem. Soc.* **2001**, *123*, 9571–9576.

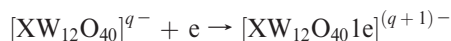
Table 3. Computed REs, RE Differences (ΔRE), and LUMO Energies for $XW_{12}O_{40}^{q-}$ Compounds in Solution

family	X	q	RE ^a	ΔRE^b	exptl ΔE°	LUMO ^c
Keggin III	B	5-	458			-3.83
	Al		373	-85	-81	-3.87
	Ga		337	-121	-104	-3.89
Keggin IV	Si	4-	191	-72	-37	-4.13
	Ge		119			-4.15
Keggin V	P	3-	0	-45	-30	-4.38
	As		-45			-4.41

^a RE, ΔRE , and ΔE° in meV. ^b ΔRE and ΔE° are relative to the first element of the same group. ^c LUMO in eV.

potential. Using the *ADF*^{20–22} program, we applied the generalized gradient approximation, applying the $X\alpha$ model with Becke's corrections^{23,24} for describing exchange and the VWN parametrization²⁵ with Perdew's corrections^{26,27} for correlation (BP86 functional). The electrons were described by Slater-type functions with basis sets of triple- ξ + polarization quality for all valence electrons. Core electrons were kept frozen and described by single Slater functions (core shells by atom: O and B, 1s; Al, Si, P, 1s2p; Ga, Ge, and As, 1s2p; W, 1s4d). We applied scalar relativistic corrections to core electrons by means of the zeroth-order regular approximation with the core potentials generated using the *DIRAC* program.²⁰ We optimized all of the geometries by using the *conductor-like screening model* (COSMO)²⁸ to account for solvent effects (water, $\epsilon = 78.4$). This specific dielectric constant mimics the media in which the present electrochemical studies have been performed. The solvent cavity surrounding the anions was created using the solvent-excluding method with fine tesserae. The ionic radii for the atoms that actually define the size of the solvent cavity were chosen to be 1.26 Å for tungsten and 1.52 Å for oxygen. We applied the spin-unrestricted formalism to open-shell species. The geometries were fully optimized within the restrictions of the maximal symmetry point groups for the oxidized and reduced species.

To compare theoretical and experimental first reduction processes, we computed the reduction energies (REs) by means of DFT calculations, shown in Table 3, for Keggin III–V compounds. The RE is defined as the energy difference between the one-electron-reduced and -oxidized forms of the Keggin anion:



Because the anion charges of the reduced and oxidized forms differ, the RE must be computed in the presence of a solvent (COSMO). Otherwise, energies would not be reliable

(20) *ADF2008.01*, SCM, Theoretical Chemistry, Vrije Universiteit, Amsterdam, The Netherlands, <http://www.scm.com>.

(21) Fonseca Guerra, C.; Snijders, J. G.; Te Velde, G.; Baerends, E. J. *Theor. Chem. Acc.* **1998**, *99*, 391.

(22) Te Velde, G.; Bickelhaupt, F. M.; van Gisbergen, S. J. A.; Fonseca Guerra, C.; Baerends, E. J.; Snijders, J. G.; Ziegler, T. *J. Comput. Chem.* **2001**, *22*, 931.

(23) Becke, A. D. *J. Chem. Phys.* **1986**, *84*, 4524.

(24) Becke, A. D. *Phys. Rev.* **1988**, *A38*, 3098.

(25) Vosko, S. H.; Wilk, L.; Nusair, M. *Can. J. Phys.* **1980**, *58*, 1200.

(26) Perdew, J. P. *Phys. Rev.* **1986**, *B33*, 8822.

(27) Perdew, J. P. *Phys. Rev.* **1986**, *B34*, 7406.

(28) (a) Klamt, A.; Schüürmann, G. *J. Chem. Soc., Perkin Trans.* **1993**, *2*, 799. (b) Andzelm, J.; Kölmel, C.; Klamt, A. *J. Chem. Phys.* **1995**, *103*, 9312.

(c) Klamt, A. *J. Chem. Phys.* **1995**, *99*, 2224. (d) Model implemented in the ADF package by: Pye, C. C.; Ziegler, T. *Theor. Chem. Acc.* **1999**, *101*, 396.

for comparison, as in the gas phase.²⁹ Not all of the REs are, in the present case, directly comparable to the experimental potentials on an equal footing because the latter are much more dependent on the media in which the CVs have been measured. We are therefore mainly motivated at reproducing and understanding the *differences* between the redox potentials. Taking RE = -4.10 eV for PW_{12} as the computational reference, we find three sets of RE values, with the correct trend: the lowest values obtained correspond to the most oxidant species (XW_{12} , X = P and As) with the lowest anion charge (3-). Intermediate and more positive RE relative values are computed for X = Si and Ge (191 and 119 meV, respectively) with an anion charge of 4- and, finally, the most positive ones (and least oxidizing species) correspond to X = B, Al, and Ga (458, 373, and 337 meV, respectively) because they carry a charge of 5-. This trend is simply attributed to the anion charge. The differences encountered within each group are, however, smaller in general and must be assigned to other factors.

The values of RE in Table 3 may be compared to the experimental pH 5 half-wave potentials (E°), shown in Table 2 (the highest RE correspond to the lowest E°). The differences computed by DFT (ΔRE) are, in absolute value, very similar to those of ΔE° ,³⁰ so DFT calculations reproduce fairly well the experimental trends. From DFT calculations, we have investigated the origin of those differences within each group. The lowest unoccupied molecular orbital (LUMO) energies (empty W-like orbitals) in compounds of the same group, where the reducing electron goes, are not the only reason for the differences encountered. Even if this could be the reason for the P/As couple (the energy difference is 30 meV), for Si/Ge, it decreases to 20 meV, whereas their mutual $\Delta RE = 72$ meV. Especially for group III compounds (X = B, Al, and Ga), where the energy differences of W orbitals are on the order of 20–30 meV from one compound to another, we discard this fact as the reason for variations in the redox potentials.

One hypothesis is based on the different electrostatic potentials created by the internal XO_4^{q-} units on their surroundings, such as the W position, where an incoming electron goes. As previously, we keep with the view^{10c,13–19} that the Keggin tungstates under consideration can be expressed as $XO_4^{q-}@W_{12}O_{36}$ and focus on the properties of the XO_4^{q-} units in order to explain the observations made on the redox potentials of the studied POMs.

The negative charge that each XO_4^{q-} anion carries, despite being formally 3-, 4-, and 5- for X belonging to groups V, IV, and III, respectively, can be considered to be somewhat smaller.³¹ In reality, some electron density is transferred from the internal XO_4 to the $W_{12}O_{36}$ cage. If the XO_4 fragment remains more charged in some cases, we could have an explanation for the different redox potentials measured. However, the computed charges on the XO_4 fragments, as observed by the authors of the present study, do not fully correlate with the REs obtained. An alternative to the fragment charges is the electrostatic potential, a property that can be mapped and is, in addition, more realistic than partial charges.

(29) López, X.; Bo, C.; Poblet, J. M. *J. Am. Chem. Soc.* **2002**, *124*, 12574–12582.

(30) The experimental E° for AsW_{12} has been estimated from other experiments because this compound is unstable in aqueous media.

(31) The charge of atoms or fragments is not observable. However, it is often used in theoretical studies to help understand some concepts.

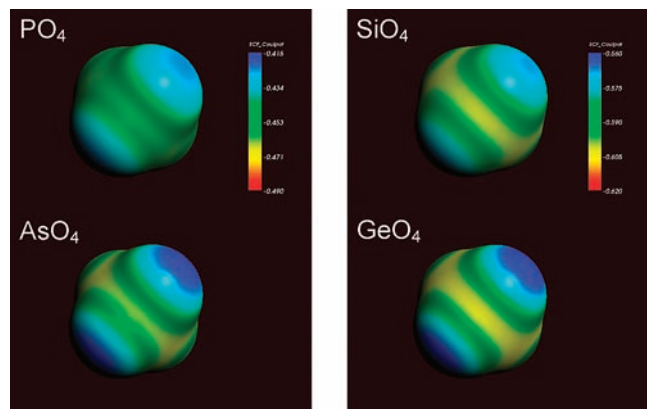


Figure 3. MEPs for XO_4^{q-} units ($X = \text{P, As, Si, and Ge}$) represented over a surface placed exactly at the $X\text{--}W$ distance. The apparent differences in the shape and extension of the surface come from the slight geometrical variations from one XO_4 to another. The potential range in each case is shown to the right in atomic units, and it changes from P--As to Si--Ge (red for more negative potentials and blue for less negative potentials). The species displaying more intense blue regions will be reduced at less negative potentials.

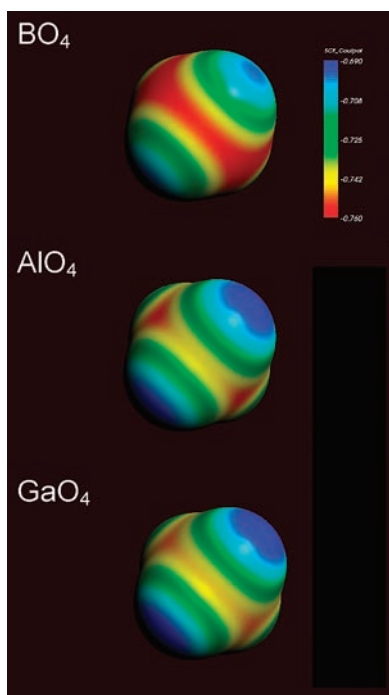


Figure 4. MEPs for XO_4^{q-} units ($X = \text{B, Al, and Ga}$) represented over a surface placed exactly at the $X\text{--}W$ distance. The potential range is shown to the right in atomic units.

A graphical representation of the molecular electrostatic potential (MEP) of XO_4^{q-} shows that some differences are appreciable for Keggin anions of the same group (MEPs for $X = \text{P, As, Si, and Ge}$ are shown in Figure 3). These representations are aimed at estimating the electrostatic potential, mapped over an isodensity surface, that the W atoms feel in the real Keggin structures.³² In this representation, blue denotes more positive potentials and red more negative ones. Thus, electrons get less destabilized around the blue regions. In the Keggin IV and V groups, the differences are small

(32) The isodensity surface has been put exactly as to contain the W atoms in it.

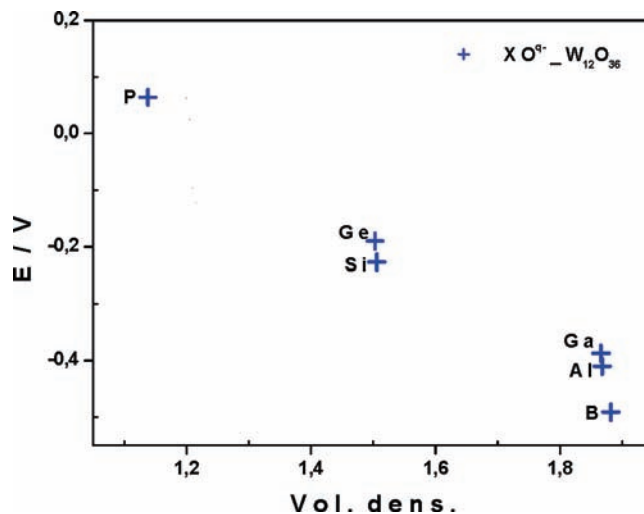
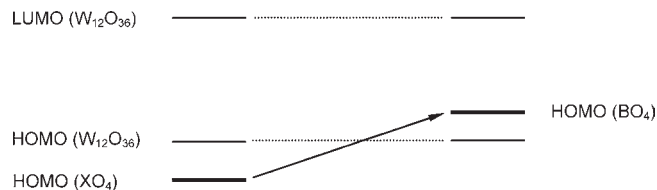


Figure 5. Apparent potential values as a function of the volumetric charge densities for different Keggin compounds. Potentials are quoted versus a SCE reference electrode.

Scheme 1



between X , in agreement with the similar redox potentials measured. Larger differences are observed within the Keggin III group (see Figure 4), where the redox potentials are more different, especially between boron and the other two heteroatoms (Al and Ga). This may be attributed to the larger electronic differences between B (second period) and the atoms from the third and fourth periods. In fact, a deeper analysis of the electronic structure of BO_4^{5-} reveals that its highest occupied molecular orbitals (HOMOs) are higher than the other XO_4^{5-} of the same group, affecting its environment in the Keggin structure. As a matter of fact, the HOMO in $\text{BO}_4^{5-}@W_{12}O_{36}$ belongs to the internal anion, a very uncommon feature when dealing with p-block heteroatoms. See Scheme 1 for a graphical representation.

We can explain this high orbital energy in connection with the small size of the BO_4^{5-} unit, the smallest of the whole series [DFT-computed equilibrium $d(X\text{--}O_{\text{tetra}}) = 1.545 \text{ \AA}$] and its high anionic charge. Similarly, in the Keggin III group, SiO_4^{4-} is more compressed than GeO_4^{4-} , featuring $d(X\text{--}O_{\text{tetra}}) = 1.653$ and 1.757 \AA , respectively. The MEP obtained for SiO_4^{4-} also shows a slight shift toward more negative potentials compared to GeO_4^{4-} , in agreement with the redox potentials obtained by cyclic voltammetry. Also, in the latter case, the SiO_4^{4-} orbitals are higher in energy than those of GeO_4^{4-} , although not to the point of being higher than the $W_{12}O_{36}$ oxo band.

For $X = \text{B}$ at least, for which the electrostatic potential is so much different compared to the other two heteroatoms of the group, we have computed the *purely* electrostatic repulsion that an incoming electron feels in the W -like LUMO without any orbital relaxation. In general, the differences are small, on the order of 70–75 meV for group IV and V heteroatoms.

X radius E° (V) $-RE$ (eV)	B 25 pm -0.491 -0.458		
	Al 53 pm -0.410 -0.373	Si 40 pm -0.227 -0.191	P 31 pm +0.064 0
	Ga 61 pm -0.387 -0.337	Ge 53 pm -0.190 -0.119	As 48 pm +0.085 +0.045

Figure 6. Shannon³³ ionic radii (pm), standard half-wave potentials (V), and $-RE$ s (eV) for the Keggin compounds labeled by their corresponding heteroatoms.

On the other hand, for group III, we found that the repulsion of an extra electron in BW_{12} is 240 meV larger than that of AlW_{12} or GaW_{12} . Even if this difference gets reduced to ca. 100 meV after orbital relaxation, it remains large, and this could explain the negative shift in the redox wave of $X = B$ versus the other two heteroatoms of the same group.

Finally, Figure 5 shows the formal redox potential values for different Keggin compounds as a function of the charge density. This graph summarizes both of the present results along with the correlation line previously established by Pope. In addition of comparisons inside the same family, it also allows for a qualitative cross-comparison between the different families of POMs studied in this work. The same general trend is observed throughout. In agreement with theoretical studies, the apparent formal potential for the first electron uptake decreases when the size of the central heteroatom decreases.

Conclusions

In summary, a pH 5 medium (0.4 M $CH_3COONa + CH_3COOH$) was found to be suitable and therefore was

selected for a comparative study of the redox properties of several heteropolytungstates. In this medium, the first cyclic voltammetric wave recorded for each compound features a one-electron, reversible process, and the electron transfer is not perturbed by protonation. Therefore, the corresponding apparent potential values, $E^\circ = (E_{pa} + E_{pc})/2$, could be used to assess the influence of the central heteroatom size on the reducibility of the POM.

DFT calculations performed on the Keggin family of compounds show that internal XO_4 units affect differently the tungstate oxide cage. We have analyzed the electrostatic potential created by each internal anionic unit in a fragment-like approach ($XO_4^{q-}@W_{12}O_{36}$) and observed that X atoms of the same group show slight differences. Within each group of the periodic table, X atoms with lower atomic numbers are also smaller in size. The net effect of such a tendency is to produce a more negative potential in the surroundings, and thus a smaller capacity to accept electrons (see the summary in Figure 6). The case of BW_{12} illustrates well this conclusion, with the smallest heteroatom of the Keggin III series and a very negative reduction potential with respect to the other elements of the same group. Particularly in this case, the electronic structure of the Keggin anion shows the effects of the small size of boron: the HOMOs of BW_{12} appear ~ 0.35 eV higher than the typical HOMOs in Keggin anions of the same charge, explaining that the BO_4 unit is more unstable than AlO_4 or GaO_4 despite carrying the same formal charge. Even if the differences in the electrostatic potentials from a qualitative level are modest, they also correlate well with the tiny differences in the experimental redox potentials.

Acknowledgment. This work was supported by the Centre National de la Recherche Scientifique (UMR 8180 and UMR 8000), Université de Versailles, Université Paris-Sud XI, Spanish MCINN (CTQ2008-06549-C02-01/BQU), Generalitat de Catalunya (2009SGR-00462), and XRTQC. X.L. thanks the Ramón y Cajal program (RYC-2008-02493).

Supporting Information Available: Cyclic voltammetric characterization of all of the POMs studied in this work, with particular emphasis on the Keggin-type compounds carrying a group III central heteroatom. This material is available free of charge via the Internet at <http://pubs.acs.org>.

(33) Shannon, R. D. *Acta Crystallogr.* **1976**, *A32*, 751.